

# Terahertz Channel Measurement and Modeling for Short-Range Indoor Environments

Ziang Zhao<sup>\*†</sup>, Weixi Liang<sup>†‡</sup>, Kai Hu<sup>†§</sup>, Qun Zhang<sup>†</sup>, Xiongbin Yu<sup>†</sup>, Qiang Li<sup>\*†</sup>

<sup>\*</sup>School of Information Science and Technology, Harbin Institute of Technology (Shenzhen), Shenzhen, China

<sup>†</sup>Department of Broadband Communication, Peng Cheng Laboratory, Shenzhen, China

<sup>‡</sup>School of Electronics and Information Technology, Sun Yat-sen University, Guangzhou, China

<sup>§</sup>School of Future Technology, South China University of Technology, Guangzhou, China

{zhaoga, liangwx02, huk02, zhangq07, yuxb, liq03}@pcl.ac.cn

**Abstract**—Accurate channel modeling is essential for realizing the potential of terahertz (THz) communications in 6G indoor networks, where existing models struggle with severe frequency selectivity and multipath effects. We propose a physically grounded Rician fading channel model that jointly incorporates deterministic line-of-sight (LOS) and stochastic non-line-of-sight (NLOS) components, enhanced by frequency-dependent attenuation characterized by optimized exponents  $\alpha$  and  $\beta$ . Unlike conventional approaches, our model integrates a two-ray reflection framework to capture standing wave phenomena and employs wideband spectral averaging to mitigate frequency selectivity over bandwidths up to 15 GHz. Empirical measurements at a 208 GHz carrier, spanning 0.1–0.9 m, demonstrate that our model achieves root mean square errors (RMSE) as low as 2.54 dB, outperforming free-space path loss (FSPL) by up to 14.2% and reducing RMSE by 73.3% as bandwidth increases. These findings underscore the importance of bandwidth in suppressing oscillatory artifacts and improving modeling accuracy. Our approach provides a robust foundation for THz system design, supporting reliable indoor wireless personal area networks (WPANs), device-to-device (D2D) communications, and precise localization in future 6G applications.

**Index Terms**—Terahertz (THz), channel measurement, channel modeling, path loss, frequency selectivity, standing wave

## I. INTRODUCTION

Terahertz (THz) band communication, spanning the frequency range from 0.1 to 10 THz [1], is anticipated to play a pivotal role in the evolution of sixth-generation (6G) wireless networks by mitigating spectrum scarcity and enabling ultra-high data rates [2]. The extensive multi-gigahertz (GHz) bandwidth available at THz frequencies underpins a wide array of transformative applications, such as multi-gigabit-per-second wireless backhaul, low-latency fronthaul for centralized radio access networks, high-speed nanoscale data exchange, immersive holographic telepresence, and networked virtual/augmented reality [1]. Furthermore, the sub-millimeter wavelengths inherent to the THz band facilitate significant transceiver miniaturization, thereby supporting innovative paradigms including wireless networks-on-chip and the Internet of Nano-Things. These advancements also propel integrated sensing and communication (ISAC), enabling high-resolution localization, environmental monitoring, and biomedical diagnostics [2]–[4].

However, harnessing THz potential is hindered by unique propagation challenges, including severe path loss, molecular

absorption, blockage susceptibility, and frequency-dependent effects like standing waves and channel sparsity [5]–[7]. Achieving terabit-per-second (Tbps) links demands ultra-wide bandwidths alongside advanced techniques such as massive multiple-input multiple-output (MIMO), intelligent reflecting surfaces, and adaptive beamforming to mitigate fading and enhance spectral efficiency [7], [8]. Accurate channel modeling, encompassing large-scale path loss and small-scale fading, is indispensable for robust transceiver design and protocol optimization [9], [10]. Addressing these challenges necessitates interdisciplinary efforts to characterize THz channels across a wide range of scenarios, including both indoor and outdoor environments, where future 6G deployments are expected [2].

Previous research on THz channel measurement and modeling has provided essential foundational insights; however, significant gaps persist, particularly above 100 GHz. Comprehensive surveys such as [1] consolidate measurement methodologies (including vector network analyzer-based frequency-domain sounding, sliding-correlation time-domain techniques, and THz time-domain spectroscopy) and modeling paradigms ranging from deterministic to stochastic and hybrid approaches. These works underscore the need for realistic propagation models tailored to 6G deployment scenarios. Indoor measurement campaigns at sub-THz frequencies (e.g., 140 GHz in office environments [5], [11]) have elucidated key channel characteristics such as path loss, delay spread, and angular statistics, frequently employing highly directional antennas to resolve multipath components (MPCs) and utilizing ray-tracing techniques for hybrid channel modeling [12]. For example, [13] extends these investigations to the 201–209 GHz band, proposing ray-tracing-statistical hybrid models for both LOS and NLOS indoor scenarios. Studies in the 240–300 GHz range have characterized short-range channels using statistical distributions to facilitate capacity analysis [14].

Higher-frequency studies, such as 300 GHz intra-wagon measurements [10], elucidate region-specific channel behaviors and align with standardized frameworks like 3GPP’s Quasi-Deterministic Radio Channel Generator (QuaDRiGa). Specialized phenomena (including standing-wave effects [6], [15], [16] and vegetation-induced shadowing [17]) have been modeled deterministically, revealing frequency-dependent resonances and channel sparsity [7]. NLOS propagation involv-

ing scattered rays and complex material interactions, such as reflection and scattering from drywall and glass surfaces [18], further emphasize the necessity for customized channel models. Device-specific studies, such as investigations into resonant tunneling diode feedback mechanisms, provide valuable insights for oscillator design in THz transceivers.

Despite notable progress, current research predominantly concentrates on frequencies below 200 GHz or investigates limited deployment scenarios, resulting in a paucity of data regarding small-scale fading characteristics at higher bands such as 208 GHz [1], [13]. Existing measurement campaigns often lack the fine-grained spatial and temporal resolution necessary to accurately capture short-range indoor channel dynamics. Furthermore, conventional models, such as those based on the 3GPP framework, tend to overestimate multipath richness while failing to adequately represent channel sparsity and the effects of standing-wave phenomena [5], [7]. Although hybrid modeling approaches [2], [12] demonstrate significant potential, their efficacy remains contingent upon validation with high-fidelity measurement datasets at frequencies above 200 GHz.

In this paper, we conduct wideband channel measurements and modeling at a 208 GHz carrier frequency in an indoor short-range environment to address critical gaps in existing THz propagation research. The primary contributions of this work are outlined as follows:

- We design and implement a sliding-correlator-based channel sounder featuring directive horn antennas, arbitrary waveform generation, 16-fold frequency multiplication from a 13 GHz local oscillator, and coherent downconversion, enabling high-resolution characterization of THz propagation characteristics.
- We capture and analyze large-scale path loss over transmitter-receiver separations of 0.1–0.9 m in 1 cm increments, along with small-scale fading over 450–453 mm in 0.05 mm steps, across a 15 GHz single-sideband (SSB) bandwidth, thereby providing a comprehensive empirical dataset for THz channel modeling.
- Leveraging the measurement dataset, we develop a hybrid frequency-selective Rician fading model that integrates deterministic LOS propagation with stochastic multipath effects, incorporating a two-ray reflection mechanism to account for standing wave phenomena.
- We conduct a detailed analysis of path loss exponents, frequency selectivity, and bandwidth effects, achieving RMSEs as low as 2.54 dB. Our results outperform FSPL benchmarks by up to 14.2%, providing valuable insights for the design of resilient 6G THz systems.

The remainder of this paper is organized as follows. In Section II, we describe the THz channel measurement platform and detail the channel measurement procedure. In Section III, the channel model is derived and frequency selectivity is discussed. Channel modeling and simulation results are presented and analyzed in Section IV, followed by conclusions in Section V.

## II. EXPERIMENTAL PLATFORM AND PROCEDURE

### A. Terahertz Platform Setup

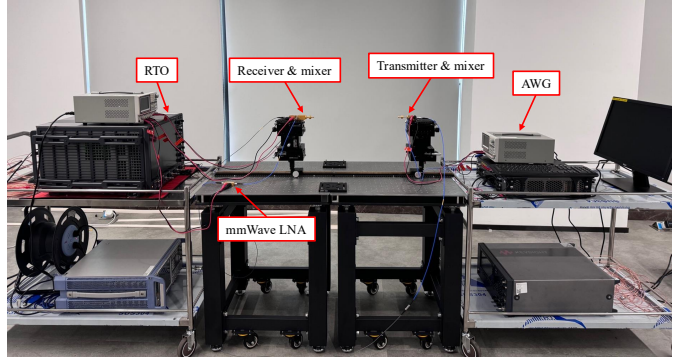


Fig. 1. Channel measurement platform

As illustrated in Fig. 1, the experimental platform consists of a transmitter (TX) and receiver (RX), each performing synchronized operations for precise signal generation, transmission, and reception in THz channel characterization.

At the TX, an arbitrary waveform generator (AWG) generates the desired baseband signal, which is subsequently upconverted to a 7.5 GHz intermediate frequency (IF). This IF signal is then fed into a sub-harmonic mixer, where it is combined with the output of an eight-fold frequency multiplier driven by a 13 GHz local oscillator (LO), resulting in a carrier frequency of 104 GHz. By exploiting the mixer's inherent nonlinearity, the second-order harmonic at 208 GHz is selectively isolated, thus achieving an effective sixteen-fold multiplication of the LO frequency. The 208 GHz signal is subsequently amplified and radiated through a horn antenna (Tx Ant) for free-space transmission.

At the RX, the THz signal is collected by a horn antenna (Rx Ant) and amplified using a terahertz low-noise amplifier (THz LNA) to improve the signal-to-noise ratio. The amplified signal is then downconverted in a sub-harmonic mixer, utilizing a frequency-multiplied LO signal that mirrors the transmitter configuration, thereby enabling coherent demodulation. The resulting IF signal is further amplified by a millimeter-wave low-noise amplifier (mmWave LNA) and digitized with a real-time oscilloscope (RTO).

Subsequent digital signal processing, as illustrated in Fig. 2, includes filtering, resampling, time-domain equalization, amplitude equalization, down-sampling, synchronization, mixing, and up-sampling. This comprehensive processing pipeline preserves the integrity and accuracy of the measured THz channel parameters, supporting robust evaluation of the wireless link.

### B. Experiment Procedure

To characterize path loss in short-range THz channels at 208 GHz, a sliding-correlation-based channel sounding system was employed in a predominantly LOS, unobstructed indoor setting. TX and RX separations were systematically varied to capture both large-scale and small-scale fading effects, with key experimental parameters summarized in Table I.

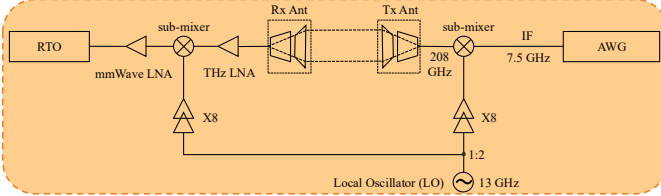


Fig. 2. Channel measurement framework

TABLE I  
EXPERIMENTAL SETUP PARAMETERS

Parameter	Symbol	Value
Carrier Frequency	$f_c$	208 GHz
Local Oscillator Frequency	$f_{LO}$	13 GHz
Start Frequency	$f_{start}$	193 GHz
Stop Frequency	$f_{stop}$	223 GHz
Bandwidth	$B_w$	15 GHz
Sampling Rate	$f_s$	256 GHz
Sampling Time	$T_s$	8.192 $\mu$ s
Maximum Delay	$\tau_{max}$	7.00 $\mu$ s
Antenna Gain	$G$	12.99 dB
Antenna HPBW	$HPBW$	21°
Modulation Type	—	Double Sideband (DSB)
Baud Rate	—	30 Baud
Signal Length	—	1 × 2097152

For large-scale path loss, the TX-RX distance was incremented from 10 cm to 90 cm in 1 cm steps (81 measurements total), while small-scale fading was assessed by varying the separation from 45.00 cm to 45.30 cm in 0.05 mm increments (61 measurements total). At each position, signals were acquired using a 208 GHz carrier and 15 GHz bandwidth, with 2,097,152 received voltage samples collected per measurement point. Received power was computed as the mean squared magnitude of these samples.

This methodology provides a comprehensive dataset for analyzing propagation dynamics in the THz band, thereby supporting subsequent channel modeling.

### III. TERAHERTZ CHANNEL MODELING AND ANALYSIS

### A. Channel Model

In this work, the wireless channel is modeled as a Rician fading channel, which accurately characterizes propagation environments with a dominant LOS path and stochastic multipath NLOS components. The complex channel coefficient is given by:

$$H = \sqrt{\frac{K}{1+K}} H_{\text{LOS}} + \sqrt{\frac{1}{1+K}} H_{\text{NLOS}}, \quad (1)$$

where  $K$  is the Rician factor representing the LOS-to-NLOS power ratio,  $H_{\text{LOS}}$  is the deterministic LOS component, and  $H_{\text{NLOS}}$  is a zero-mean complex Gaussian variable modeling aggregated scattered paths. This normalization ensures unit average power and provides a versatile framework for THz channel analysis, with Rayleigh fading ( $K = 0$ ) and pure LOS ( $K \rightarrow \infty$ ) as special cases.

### B. Frequency Selectivity

The LOS component models attenuation as a function of both frequency and TX-RX separation:

$$H_{\text{LOS}} = \frac{c}{4\pi f_c^\alpha d^\beta} e^{-j\frac{2\pi f_c d}{c}}, \quad (2)$$

where  $c$  is the speed of light,  $f_c$  is the carrier frequency, and  $d$  is the separation distance. The exponents  $\alpha$  and  $\beta$  capture frequency selectivity and distance-dependent attenuation, respectively, fitted empirically via least-squares minimization:

$$(\hat{\alpha}, \hat{\beta}) = \arg \min_{\alpha, \beta} \sum_i \left| \text{PL}_i + 20 \log_{10} \left( \frac{c}{4\pi f_{c,i}^{\alpha} d_i^{\beta}} \right) \right|^2, \quad (3)$$

with  $PL_i$  denoting measured path loss at  $f_{c,i}$  and  $d_i$ . The corresponding path loss is:

$$\text{PL}(d) = -20 \log_{10} |H_{\text{LOS}}| = 20 \log_{10} \left( \frac{4\pi f_c^{\alpha} d^{\beta}}{c} \right). \quad (4)$$

Substituting (2) into (1) gives the full response, enabling data-driven modeling of THz phenomenology, as validated in subsequent results.

### C. Analytical Solution for Wideband Channels

For wideband channels, the frequency-selective response is integrated over the operational bandwidth to derive an averaged channel model. This integration is expressed as

$$I(A, B, \alpha, \tau) = \frac{c}{4\pi d^\beta} \int_B^A f^{-\alpha} e^{-j2\pi f\tau} df, \quad (5)$$

where  $\tau = d/c$  represents the time delay, and the integration bounds  $B$  and  $A$  define the frequency spectrum (e.g., 193 GHz to 223 GHz for a 208 GHz carrier frequency with a 15 GHz baseband). To facilitate analytical evaluation, the integral is transformed via the substitution  $u = -j2\pi f\tau$ , resulting in

$$I(A, B, \alpha, \tau) = \frac{c}{4\pi d^\beta} (-j2\pi\tau)^{\alpha-1} \int_{u(B)}^{u(A)} \frac{e^u}{u^\alpha} du. \quad (6)$$

This form can be evaluated using the generalized exponential integral, defined as  $E_\alpha(z) = \int_z^\infty u^{\alpha-1} e^{-u} du$ . The analytical solution enables efficient parameter optimization by minimizing discrepancies between the model and empirical wide-band measurements. This approach effectively accounts for bandwidth-dependent frequency selectivity, as corroborated by the empirical results, thereby enhancing the model's accuracy and applicability in THz system simulations.

#### D. Small-Scale Fading and Two-Ray Model

Small-scale fading, such as standing waves from multipath interference, is integrated via the NLOS term or explicitly modeled using a two-ray approximation method for reflective environments:

$$H_{\text{two-ray}} = \frac{c}{4\pi f_c d} e^{-j\frac{2\pi f_c d}{c}} + \Gamma \frac{c}{4\pi f_c d'} e^{-j\frac{2\pi f_c d'}{c}}, \quad (7)$$

where  $d'$  is the reflected path length and  $\Gamma$  is the reflection coefficient. This form captures periodic fluctuations, which can be generalized with tunable parameters (e.g., cosine terms) for optimization against measurements, as detailed in the results.

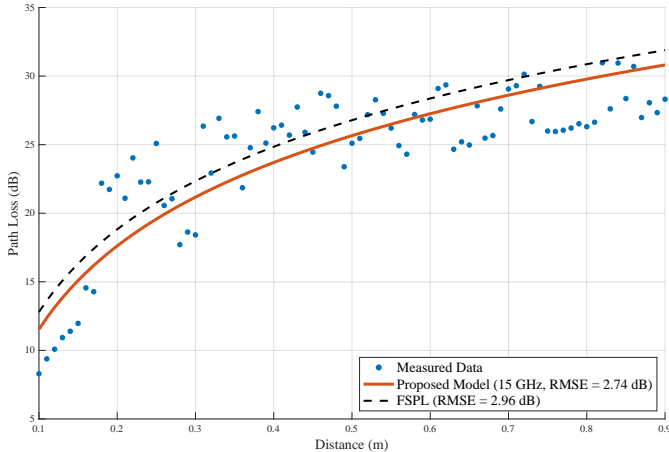


Fig. 3. Comparison of measured path loss with the proposed model (15 GHz bandwidth) and FSPL benchmark at 208 GHz carrier frequency.

#### IV. RESULTS

This section presents a comprehensive empirical validation and quantitative assessment of THz wideband channel characteristics measured at 208 GHz. Our analysis encompasses path loss modeling, small-scale fading, standing wave effects, and frequency selectivity, demonstrating significant advancements in THz channel characterization. The proposed hybrid model achieves RMSEs as low as 2.54 dB, representing a 14.2% improvement over conventional FSPL models. These findings provide critical insights for short-range indoor THz propagation and establish a foundation for robust 6G system design.

##### A. Performance of the Proposed Path Loss Model

The proposed path loss model is an enhanced Rician fading framework tailored for THz communications, which integrates a deterministic LOS component with stochastic NLOS contributions to capture the complex propagation dynamics at sub-millimeter wavelengths. Specifically, the model accounts for frequency-dependent attenuation through parameters  $\alpha$  (frequency-dependent exponent) and  $\beta$  (distance scaling exponent), while incorporating small-scale fading effects via a two-ray reflection mechanism to model standing wave phenomena.

To address wideband frequency selectivity, the frequency-selective response is averaged over the operational bandwidth, as detailed in (5). The NLOS component,  $H_{\text{NLOS}}$ , is modeled as a zero-mean complex Gaussian process, contributing to the overall Rician distribution that characterizes the channel's fading behavior. Parameters such as  $\alpha$ ,  $\beta$ , and  $K$  factor are optimized via least-squares fitting against empirical data to minimize discrepancies.

Fig. 3 illustrates the path loss characteristics measured over distances from 0.1 m to 0.9 m at 208 GHz. The proposed model, optimized across a 15 GHz baseband bandwidth (corresponding to 193–223 GHz in double-sideband transmission), achieves a RMSE of 2.74 dB compared to the measured data. This represents a 0.22 dB improvement over the FSPL

TABLE II  
PATH LOSS MODEL PERFORMANCE ACROSS BANDWIDTHS AT 208 GHz CARRIER FREQUENCY

BW (GHz)	RMSE (dB)	Improvement vs. FSPL (dB)	Calibration Constant $C$
0.5	9.17	-6.22	13.34
1	9.30	-6.35	12.35
5	2.89	0.07	9.06
10	2.82	0.14	11.09
15	2.74	0.22	-0.11

benchmark (RMSE = 2.96 dB), demonstrating the model's enhanced ability to capture frequency-selective propagation phenomena and multipath effects inherent in THz channels.

Table II quantifies the model performance across various bandwidths. Narrowband configurations (0.5 GHz and 1 GHz) exhibit significantly higher RMSEs (9.17 dB and 9.30 dB, respectively), attributed to insufficient spectral averaging of frequency-dependent channel variations. Conversely, wider bandwidths demonstrate progressive RMSE reduction, with the 15 GHz configuration achieving optimal accuracy. The bandwidth-dependent calibration constant  $C$  indicates the necessity for adaptive parameterization in practical implementations.

The model demonstrates superior fidelity particularly beyond 0.3 m, where FSPL systematically overestimates path loss due to its inability to account for multipath interference and frequency-selective effects. These results validate the necessity for empirically-driven modeling approaches in THz channel characterization, where conventional free-space models fail to capture the complex propagation dynamics.

##### B. Standing Wave Effects and Small-Scale Fading

Small-scale fading arising from multipath interference significantly impacts THz propagation in indoor environments. To investigate these phenomena, we analyzed path loss variations over a 3 mm range (450–453 mm) with 0.05 mm step size. The two-ray reflection model described in (7) was employed to characterize standing wave patterns resulting from constructive and destructive interference between direct and reflected signal components.

Fig. 4 illustrates the bandwidth-dependent behavior of small-scale fading. As shown in Table III, model fitting accuracy improves monotonically with increasing bandwidth, with RMSE decreasing from 2.21 dB at 0.5 GHz to 0.59 dB at 15 GHz (a 73.3% reduction). This improvement results from the inherent frequency diversity of wideband signals, which effectively averages out frequency-selective fading components and produces more stable channel characteristics.

These findings have significant implications for THz system design, particularly for applications requiring precise channel state information, such as beamforming, localization, and ultra-reliable low-latency communications. The demonstrated bandwidth-dependent fading suppression provides a practical design guideline for mitigating small-scale channel variations in future 6G deployments.

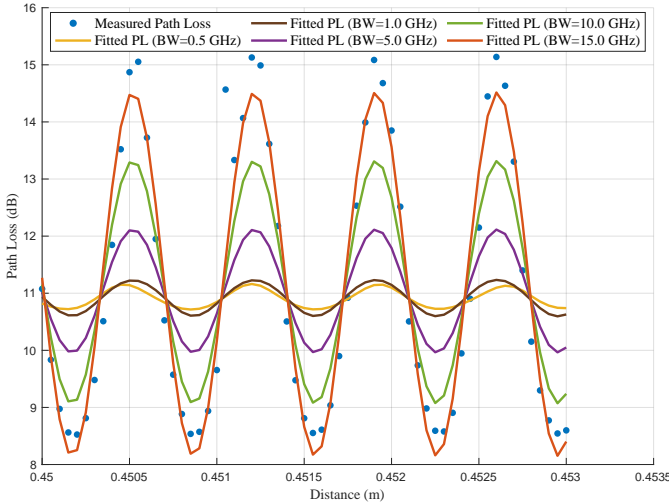


Fig. 4. Path loss fitting using the two-ray model across different bandwidths at 208 GHz, demonstrating the impact of bandwidth on small-scale fading characteristics.

TABLE III  
TWO-RAY MODEL FITTING ACCURACY ACROSS BANDWIDTHS

Bandwidth (GHz)	RMSE (dB)
0.5	2.21
1.0	2.13
5.0	1.62
10.0	0.96
15.0	0.59

### C. Integrated Path Loss Modeling with Standing Wave Effects

To develop a comprehensive channel model, we integrated the large-scale path loss component with small-scale standing wave effects. This hybrid approach captures both distance-dependent attenuation and periodic spatial variations, providing a more accurate representation of THz propagation than conventional models. Building on the two-ray approximation detailed in (7), which models multipath interference through direct and reflected paths, the standing wave effects manifest as periodic fluctuations in the received signal strength. For practical optimization in simulations, these effects are generalized and incorporated as a cosine-modulated term, which approximates the interference pattern while allowing tunable parameters to fit empirical data effectively. The integrated model is thus expressed as:

$$PL(d) = 20 \log_{10} \left( \frac{4\pi f_c^\alpha d^\beta}{c} \right) + A \cos \left( \frac{2\pi d}{\lambda} + \phi \right) + C, \quad (8)$$

where  $A$ ,  $\phi$ , and  $C$  represent the standing wave amplitude, phase offset, and overall calibration constant, respectively, obtained through least-squares optimization.

Fig. 5 demonstrates the performance of the integrated model for a 15 GHz bandwidth configuration. The model achieves an RMSE of 2.54 dB, representing improvements of 7.3% and 14.2% over the large-scale-only model (2.74 dB) and FSPL (2.96 dB), respectively. As shown in Table IV, consistent

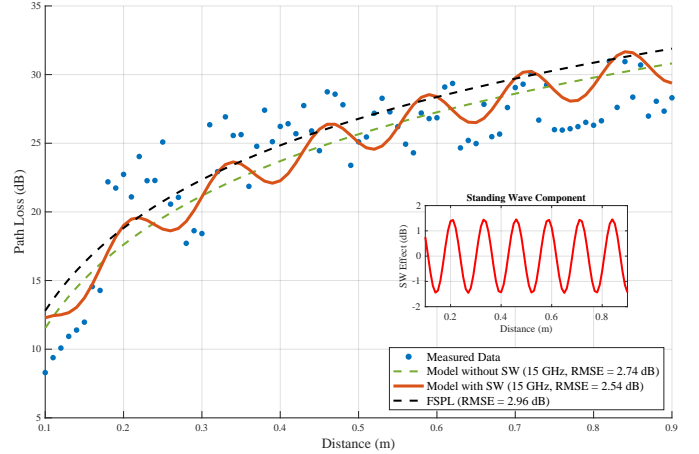


Fig. 5. Integrated path loss model incorporating standing wave effects (15 GHz bandwidth). The inset shows the isolated standing wave component contribution.

RMSE reductions are observed across all evaluated bandwidths, highlighting the effectiveness of incorporating standing wave dynamics in THz channel modeling.

TABLE IV  
RMSE COMPARISON: IMPACT OF STANDING WAVE (SW) INTEGRATION

BW (GHz)	RMSE w/o SW (dB)	RMSE with SW (dB)	Improvement (%)
0.5	9.17	6.02	34.39
1.0	9.30	8.40	9.70
5.0	2.89	2.76	4.46
10.0	2.82	2.76	1.87
15.0	2.74	2.54	7.30

The integrated model provides a physically motivated framework that bridges macro- and micro-scale propagation phenomena, offering enhanced accuracy for THz channel prediction and system-level performance evaluation.

### D. Channel Frequency Selectivity and Bandwidth Effects

THz channels exhibit pronounced frequency selectivity arising from molecular absorption, scattering, and multipath propagation. Our analysis quantifies the extent to which increasing bandwidth mitigates these effects via spectral diversity, offering critical insights for spectrum allocation and waveform design in THz communications.

Fig. 6 illustrates the impact of measurement bandwidth on path loss modeling accuracy over the 0.1 to 0.9 m range at 208 GHz. The 15 GHz bandwidth configuration achieves the lowest RMSE of 2.74 dB, exhibiting a smooth path loss trend that closely follows the measured data. In contrast, narrower bandwidth configurations suffer from substantial modeling errors, with the 1 GHz bandwidth reaching an RMSE of 15.36 dB, due to unresolved frequency-selective fading. The pronounced oscillations (crests and troughs) observed in the narrowband models are a result of multipath-induced constructive and destructive interference. The wider 15 GHz bandwidth

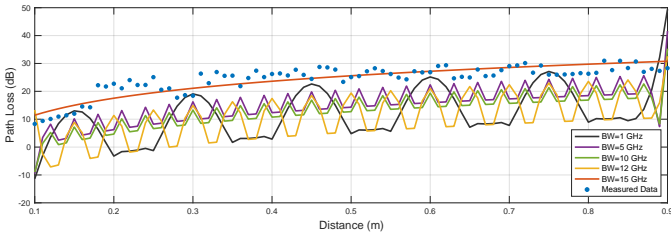


Fig. 6. Bandwidth impact on path loss modeling accuracy at 208 GHz. Wider bandwidths demonstrate improved model fidelity through frequency diversity gain.

effectively averages out these fluctuations through frequency diversity gain, which suppresses the crests and troughs and significantly improves model fidelity.

These results demonstrate that wideband operation not only enhances spectral efficiency but also significantly improves channel predictability and modeling accuracy. The observed 14.2% improvement over conventional models, together with the quantified bandwidth-dependent performance, provides essential design guidelines for future THz communication systems and supports the development of robust and efficient 6G wireless networks.

## V. CONCLUSION

This paper presents an enhanced path loss modeling framework for THz communications at 208 GHz, effectively integrating large-scale attenuation with small-scale standing wave effects to address the complexities of short-range indoor propagation. The empirical results demonstrate that wideband modeling is essential for capturing intricate propagation mechanisms at sub-millimeter wavelengths, where environmental interactions extend beyond mere geometric spreading and introduce significant frequency selectivity and multipath interference. The proposed model's close alignment with measured data, achieving RMSEs as low as 2.54 dB and outperforming FSPL benchmarks by up to 14.2%, validates the critical role of parameters such as frequency-dependent decay ( $\alpha$ ), distance scaling ( $\beta$ ), and the Rician factor in representing dominant THz channel characteristics. Moreover, the observed improvement in fitting accuracy with increasing bandwidth emphasizes the need for bandwidth-aware optimization strategies to enhance model performance.

Future research could extend this framework by incorporating dynamic environmental variables, such as humidity and obstacle density, to better simulate real-world variability. Additionally, exploring adaptive bandwidth selection and advanced techniques, including machine learning-based parameter estimation, may further improve the model's generalizability and precision across diverse THz scenarios, ultimately supporting the development of robust 6G and beyond systems.

## ACKNOWLEDGMENT

This work acknowledges the support from the National Science and Technology Major Project – Mobile Information Networks under Grant No. 2025ZD1303200.

## REFERENCES

- C. Han, Y. Wang, Y. Li, Y. Chen, N. A. Abbasi, T. Kürner, and A. F. Molisch, "Terahertz wireless channels: A holistic survey on measurement, modeling, and analysis," *IEEE Communications Surveys & Tutorials*, vol. 24, no. 3, pp. 1670–1707, 2022.
- K. Guan, H. Yi, D. He, B. Ai, and Z. Zhong, "Towards 6g: Paradigm of realistic terahertz channel modeling," *China Communications*, vol. 18, no. 5, pp. 1–18, 2021.
- W. Jiang, Q. Zhou, J. He, M. A. Habibi, S. Melnyk, M. El-Absi, B. Han, M. D. Renzo, H. D. Schotten, F.-L. Luo, T. S. El-Bawab, M. Juntti, M. Debbah, and V. C. M. Leung, "Terahertz communications and sensing for 6g and beyond: A comprehensive review," *IEEE Communications Surveys & Tutorials*, vol. 26, no. 4, pp. 2326–2381, 2024.
- K. Hu, L. Zou, M. Luo, J. Jiang, and R. Li, "Wireless channel modeling for viewpoint and trajectory planning in aerial coverage exploration," in *2025 IEEE International Conference on Communications Workshops (ICC Workshops)*, 2025, pp. 141–146.
- Y. Xing, T. S. Rappaport, and A. Ghosh, "Millimeter wave and sub-thz indoor radio propagation channel measurements, models, and comparisons in an office environment," *IEEE Communications Letters*, vol. 25, no. 10, pp. 3151–3155, 2021.
- H. Tran, T. Le, and S. Singh, "Effect of standing wave on terahertz channel model," in *2021 IEEE International Conference on Communications Workshops (ICC Workshops)*, 2021, pp. 1–6.
- X. Liu, J. Zhang, P. Tang, L. Tian, H. Tataria, S. Sun, and M. Shafi, "Channel sparsity variation and model-based analysis on 6, 26, and 105 ghz measurements," *IEEE Transactions on Vehicular Technology*, vol. 73, no. 7, pp. 9387–9397, 2024.
- D. Bodet, P. Dinh, M. Stojanovic, J. Widmer, D. Koutsonikolas, and J. M. Jornet, "Characterizing sub-thz mimo channels in practice: a novel channel sounder with absolute time reference," in *GLOBECOM 2023 - 2023 IEEE Global Communications Conference*, 2023, pp. 1459–1464.
- A. Goldsmith, *Wireless Communications*. Cambridge, UK: Cambridge University Press, 2005.
- K. Guan, B. Peng, D. He, J. M. Eckhardt, S. Rey, B. Ai, Z. Zhong, and T. Kürner, "Channel characterization for intra-wagon communication at 60 and 300 ghz bands," *IEEE Transactions on Vehicular Technology*, vol. 68, no. 6, pp. 5193–5207, 2019.
- Y. Chen, C. Han, Z. Yu, and G. Wang, "140 ghz channel measurement and characterization in an office room," in *ICC 2021 - IEEE International Conference on Communications*, 2021, pp. 1–6.
- Y. Chen, Y. Li, C. Han, Z. Yu, and G. Wang, "Channel measurement and ray-tracing-statistical hybrid modeling for low-terahertz indoor communications," *IEEE Transactions on Wireless Communications*, vol. 20, no. 12, pp. 8163–8176, 2021.
- Y. Chen, C. Han, Z. Yu, and G. Wang, "Channel measurement, characterization, and modeling for terahertz indoor communications above 200 ghz," *IEEE Transactions on Wireless Communications*, vol. 23, no. 6, pp. 6518–6532, 2024.
- E. Karakoca, H. Nayir, G. K. Kurt, and A. Görçin, "Measurement-based modeling of short range terahertz channels and their capacity analysis," in *GLOBECOM 2023 - 2023 IEEE Global Communications Conference*, 2023, pp. 1471–1476.
- A. Semenova, A. Yablokov, V. Anfertev, and T. Knyazeva, "The influence of the standing-wave interference in the cell on the gas spectroscopy measurements in the thz range," in *2022 IEEE 8th All-Russian Microwave Conference (RMC)*, 2022, pp. 353–356.
- H. Jalili and O. Momeni, "A standing-wave architecture for scalable and wideband millimeter-wave and terahertz coherent radiator arrays," *IEEE Transactions on Microwave Theory and Techniques*, vol. 66, no. 3, pp. 1597–1609, 2018.
- A. Afsharinejad, A. Davy, B. Jennings, S. Rasmann, and C. Brennan, "A path-loss model incorporating shadowing for thz band propagation in vegetation," in *2015 IEEE Global Communications Conference (GLOBECOM)*, 2015, pp. 1–6.
- Y. Xing, O. Kanhere, S. Ju, and T. S. Rappaport, "Indoor wireless channel properties at millimeter wave and sub-terahertz frequencies," in *2019 IEEE Global Communications Conference (GLOBECOM)*, 2019, pp. 1–6.